Quantization in magnetoresistance
of strained InSb whiskers

A. Druzhinin[1,2], I. Ostrovskii[1,2], Yu. Khoverko[1,2], and N. Liakh-Kaguy[1]

[1]*Lviv Polytechnic National University, 12 S. Bandera Str., Lviv 79013, Ukraine*

[2]*Institute of Low Temperature and Structure Research PAS, 95 Gajowicka, Wroclaw, Poland*
E-mail: druzh@polynet.lviv.ua

Strain influence on the longitudinal magnetoresistance for the *n*-type conductivity InSb whiskers doped by Sn to concentration $6\cdot10^{16}$–$6\cdot10^{17}$ cm^{-3} was studied in the temperature range 4.2–40 K and magnetic field up to 10 T. The Shubnikov–de Haas oscillations at low temperatures were observed in the strained and unstrained samples in all range of doping concentrations and magnetic fields. The character of longitudinal magnetoresistance dependences was analyzed and compared with theoretical one. The whisker magnetoresistance alters its sign with increasing magnetic field. It is positive at weak magnetic fields and becomes negative at higher magnetic fields. Possible mechanism of the large value of negative magnetoresistance (NMR) was discussed in the InSb whiskers with doping concentration in the vicinity to metal–insulator transition. The origin of large NMR was explained by the existence of classical size effect and boundary scattering during conductance in subsurface whisker layers.

Keywords: InSb whiskers, negative longitudinal magnetoresistance, doping concentration, strain influence.

1. Introduction

The magnetotransport measurements were carried out in InSb at low temperatures [1,2]. The hopping conduction of InSb at temperature down to 0.37 K and magnetic fields up to 7 T were interpreted in terms of electron localization in work [1]. Carrier quantum lifetime of the doped quantum well on the base of InSb was found by studying of Shubnikov–de Haas oscillations at an extremely low temperature of 2 K and weak magnetic field of 0.8 T in the modern article [2].

Different structures on the base of InSb material with narrow bandgap could be used for electronic device applications due to their high electron mobility, peak velocities and, as a result, small electron effective mass [3,4]. The high velocities of antimonide-based compound semiconductors were observed in the analog electronic devices with low power consumption at low electric fields [4].

It is interesting to study the strain influence on the magnetic properties and parameters of the InSb structures [5–9]. The influence of the biaxial compressive strain provides the decreasing of the hole effective mass obtained at cyclotron resonance measurements at temperature 4.2 K in InSb quantum wells that is in agreement with theoretical data [5]. The influence of the strain effect was studied in InSb-on-insulator devices [6–9]. A hole mobility was calculated accounting for optical and acoustic phonons and the surface roughness scattering [6]. The compressive strain is favorable to the hole mobility, in particular, the splitting the heavy- and light-hole valence bands due to strain in III–V compounds [7–9]. Compressively-strained bulk InSb demonstrated the highest hole mobility close to 1000 cm^2/(V·s) at room temperature [7].

Negative magnetoresistance (NMR) corresponding to different mechanisms of charge carrier scattering was found in such material as InSb at weak magnetic fields and low-temperature range [10–19]. NMR phenomena with strong spin-orbital coupling gaps were revealed in topological semimetals [10]. The NMR with various its interpretations was revealed in InSb structures on GaAs substrates [11,12]. NMR effect was studied in InSb layers with low thickness epitaxially grown on GaAs as a result of weak localization (WL) of charge carriers on defects near InSb/GaAs interface. Negative component of magnetoresistance arises due to scattering of the conduction electrons from localized impurity magnetic moments [11]. The authors [12] studied the NMR in the InSb film with a thickness of 0.1–1 μm in the extremely weak magnetic field and the spin-orbital scattering has been analyzed due to the bulk inversion asymmetry. And the NMR crossovers to the positive MR that corresponds to crossover from weak localization (WL) to the weak anti-localization (WAL) according to the increasing of

spin-orbital interaction in Sn-doped InSb films due to increasing of the Rashba electric field influence [12]. The NMR was also found in *n*-type conductivity InSb at temperature 77 K in the longitudinal magnetic field up to 1.8 T and its dependences on carrier concentration and mobility were studied in work [13]. Negative longitudinal magnetoresistance disappears with increasing carrier concentration due to ionized impurity scattering and crystal inhomogeneity.

The presence of magnetic ordering in InSb thin films due to introducing of the magnetic impurities such as Mn actually leads to the observation of NMR in the field dependences of the magnetoresistance [14–19]. NMR phenomena along with the Shubnikov–de Haas oscillation effect was also found in InSb whiskers with a doping concentration of Sn in the vicinity to metal–insulator transition (MIT) from metal and insulator side of the transition at magnetic field up to 10 T in the temperature range 4.2–77 K [20,21].

We already have found strain-induced Berry phase and splitting of the Shubnikov–de Haas oscillations due to the studying of the longitudinal magnetoresistance in *n*-type conductivity InSb whiskers at low temperatures [22]. The effective electron mass and Dingle temperature under compressive strain were also studied in these samples. The strain influence on the behavior of NMR wasn't analyzed in the InSb whiskers, but we have great experience in the studying strain effect on magnetoresistance of Si, Ge and SiGe solid solution whiskers at low temperatures [23–26]. Therefore, the aim of the article is magnetoresistance studying for InSb whiskers with Sn doping concentration that corresponds metal and insulator side of the MIT under compressive strain.

2. Experimental procedure

The *n*-type conductivity of InSb whiskers with different doping concentration grown by the method of chemical transport reactions were the objects for investigations of the longitudinal magnetoresistance. The whiskers with the length of 2–3 mm and diameter of 30–40 μm were used for these studies. The Au contacts to InSb whiskers with a diameter 10 μm form a eutectic with the crystals under pulsed welding. This technique of contact creation allows the measuring of the longitudinal magnetoresistance with using four contacts to studied sample.

The *n*-type conductivity InSb whiskers were strained thanks to crystal mounting on the substrates with thermal expansion coefficient that is different from InSb material. The authors of the work [25] showed the similar experimental technique with the using of thermal strain estimation for *p*-type silicon microcrystals on different substrates. The copper substrate was used to achieve a uniaxial compressive strain ($\varepsilon = -3.8 \cdot 10^{-3}$ rel. units) at 4.2 K. Thermal compressive strain in a direction $\langle 111 \rangle$ was calculated in the InSb whiskers at temperature 4.2–40 K.

The low-temperature magnetoresistance studying of InSb whiskers was carried out in a helium cryostat cooled to the temperature 4.2 K. The magnetic properties of the samples were investigated in the magnetic field 0–10 T due to use the Bitter magnet with a time of scanning 1.75 T/min. Stabilized electric current 1–10 mA was selected depending on sample resistance and created by Keithley 224 source. The temperature was measured with using the Cu–CuFe thermocouple.

3. Experimental results and their discussions

Some groups of unstrained and strained InSb whiskers with tin concentration corresponding to various approximations to the critical concentration of metal–insulator transition were studied in parallel magnetic fields with intensity 0–10 T:

(i) doping concentration corresponding to MIT — $2 \cdot 10^{17}$ cm^{-3};

(ii) doping concentration corresponding to the metal side of MIT — $6 \cdot 10^{17}$ cm^{-3};

(iii) doping concentration corresponding to insulator side of MIT — $6 \cdot 10^{16}$ cm^{-3}.

The longitudinal magnetoresistance of *n*-type conductivity InSb whiskers was investigated under uniaxial strain influence in the temperature range 4.2–40 K. The comparison of the behavior for the magnetoresistance field dependences at liquid helium temperature and various doping concentrations was shown in Fig. 1.

It is obvious from Fig. 1 that longitudinal magnetoresistance of InSb whiskers has nonmonotonic character. The values of magnetic field induction at liquid helium temperature were found, when the strained longitudinal magnetoresistance crosses *B* axis and changes sign from positive to negative and in the opposite direction. These values are different for various tin concentration and correspond to 7 and 11 T for the sample with doping concentration $6 \cdot 10^{16}$ cm^{-3} (see Fig. 1(b), curve *1*) and 5 and 7 T — for $2 \cdot 10^{17}$ cm^{-3} (Fig. 1(b), curve *2*), respectively. The other behavior of the magnetoresistance was observed in highly doped InSb whiskers with doping concentration corresponding to the metal side of MIT under strain influence at 4.2 K (Fig. 1(b), curve *3*). It doesn't change the sign and is positive up to 10 T.

It is interesting to compare the magnetoresistance dependences in strained and unstrained samples with the same tin concentration. Therefore, the longitudinal magnetoresistance for unstrained samples doped to a concentration corresponding to MIT changes the sign only one time at the magnetic field induction 4 T (Fig. 1(a), curve *2*); with doping concentration corresponding to insulator side of MIT — twice times: at 6 and 9 T (Fig. 1(a), curve *1*) and with concentration corresponding to metal side — three times (Fig. 1(a), curve *3*).
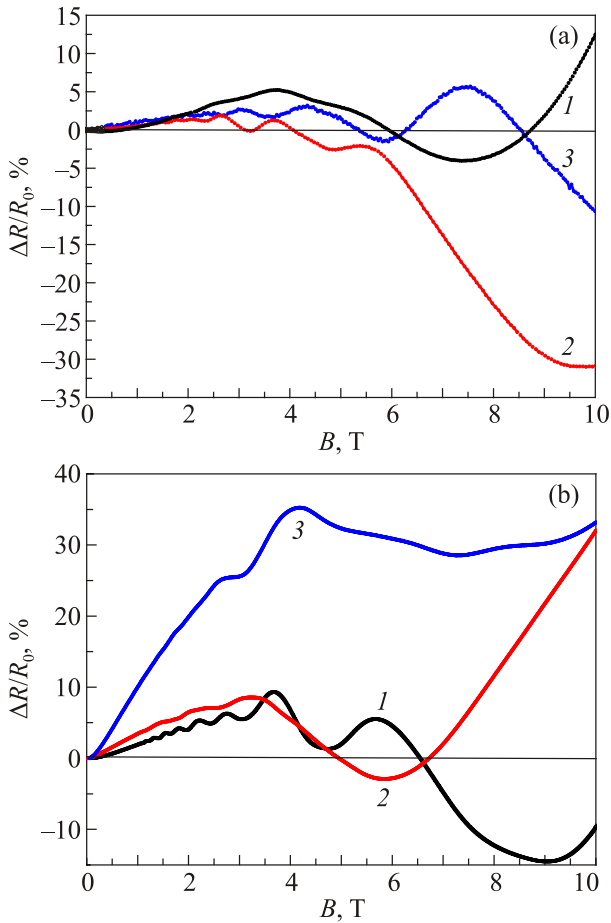
Fig. 1. (Color online) Longitudinal magnetoresistance in un-strained (a) and strained (b) InSb whiskers at 4.2 K with various tin concentration, cm^{-3}: 6·10^{16} (*1*); 2·10^{17} (*2*); 6·10^{17} (*3*).

The Shubnikov–de Haas oscillations at low temperatures were revealed in the strained and unstrained samples with all range of doping concentration that was already observed for unstrained InSb whiskers in [21]. Magnetoresistance peaks correspond to transitions between Landau levels with $N = 1, 2, \ldots$. Their number decreases from nine peaks to six for unstrained and strained samples with tin concentration corresponding to MIT, respectively (Figs. 1(a),(b), curves *2*). A number of the peaks consists of 5 in both unstrained and strained InSb whiskers with tin concentration corresponding to the metal side of MIT (Figs. 1(a),(b), curves *3*) and also for unstrained samples with tin concentration removed into insulator side of MIT (Fig. 1(a), curve *1*). For the strained samples with the same doping concentration peak number increases to nine (Fig. 1(b), curve *1*).

Therefore, strain influence leads to change of longitudinal magnetoresistance peak number (Fig. 1). Samples with doping concentration 2·10^{17} cm^{-3} were shifted from MIT under uniaxial compressive strain which leads to a decrease of peak number. For InSb whiskers slightly doped to concentration 6·10^{16} cm^{-3} peak number increases under strain that also shifts it to MIT.

The maximum peak amplitude decreases with temperature increasing in the whole range of magnetic field up to 10 T and the Shubnikov–de Haas oscillations are almost absent. The magnetoresistance of strained and unstrained InSb whiskers with different doping concentrations corresponding various approximation to MIT at temperature 40 K was presented in Fig. 2.

Strain influence on NMR parameters of *n*-type conductivity InSb whiskers at temperature 4.2 K was analyzed
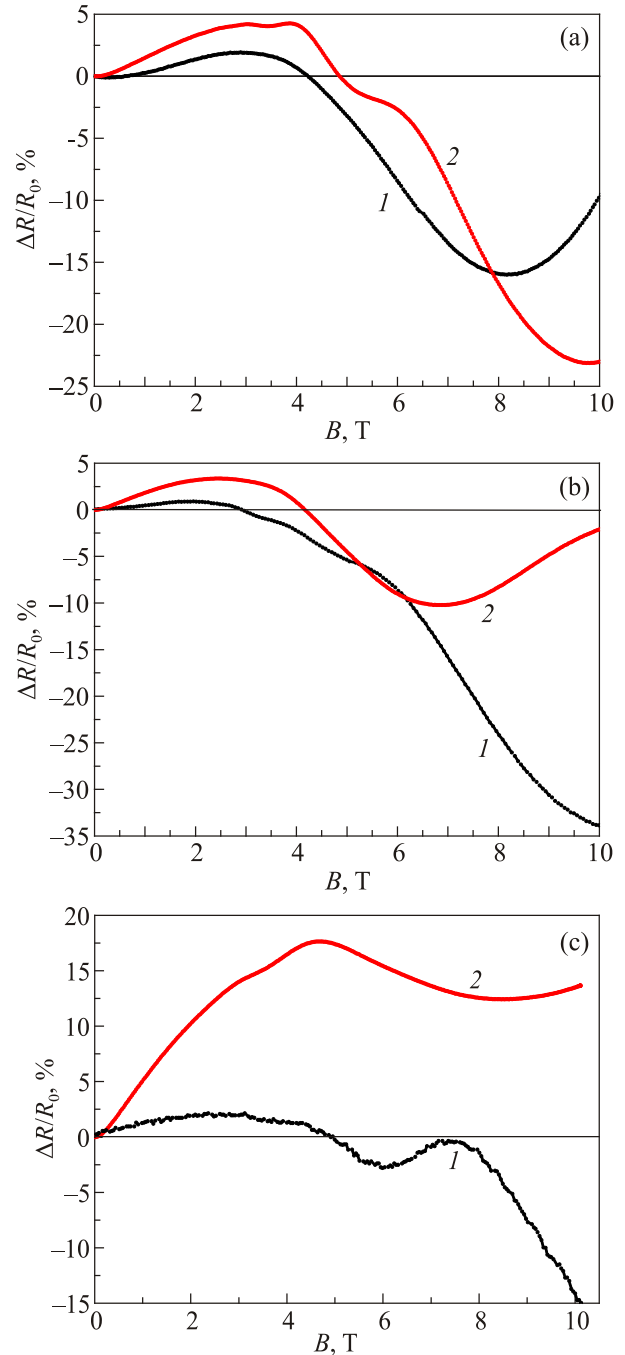

Fig. 2. (Color online) Longitudinal magnetoresistance of InSb whiskers with tin concentration 6·10^{16} (a), 2·10^{17} (b), and 6·10^{17} (c) cm^{-3} for unstrained (*1*) and strained (*2*) samples at 40 K.

and shown in Table 1. We take into account such two characteristic parameters:

(i) NMR maximum value;

(ii) critical magnetic field, when longitudinal magneto-resistance changes sign from positive to negative.

Table 1. NMR parameters of InSb whiskers with a different doping concentration at 40 K

Sample	Doping concentration, cm^{-3}	B_{cr}, T	Maximum NMR, %
Unstrained	$6 \cdot 10^{16}$	8	17
	$2 \cdot 10^{17}$	10	35
	$6 \cdot 10^{17}$	12	20
Strained	$6 \cdot 10^{16}$	10	23
	$2 \cdot 10^{17}$	7	10
	$6 \cdot 10^{17}$	–	–

As we can see from Table 1, the absolute value of the NMR at temperature 40 K is maximal (35%) for unstrained samples with tin concentration corresponding to MIT, while it significantly decreases to 10% under uniaxial compressive strain. But, for slightly doped samples with tin concentration corresponding to insulator side of MIT, the NMR consists of 23% for strained and 17% for unstrained samples. NMR is absolutely absent in strained samples with tin concentration removed into metal side of MIT, but it is very large (about 20%) for unstrained InSb whiskers.

The critical magnetic field of the longitudinal magneto-resistance increases in higher doped unstrained samples, but it decreases in strained InSb whiskers and NMR is completely absent for samples heavily doped to concentration $6 \cdot 10^{17}$ cm^{-3}. Therefore, strain influence on longitudinal magnetoresistance dependences of *n*-type conductivity InSb whiskers manifests in the reduction of the NMR effect. The critical magnetic field decreases for strained samples with tin concentration corresponding to MIT, but it increases in samples doped to a concentration of insulator side due to strain influence.

To describe the nonmonotonic character of longitudinal magnetoresistance let us consider three-dimensional quantum subband electrons. Three electron subbands (the insert of Fig. 3) were under the consideration. The parabola (*1*) corresponded to the lowest states ($N_1 = N_2 = 0$), while parabola (*2*) represented first size quantized zone ($N_1 = 0$; $N_2 = 1$), parabola (*3*) was described by quantum numbers ($N_1 = 1$; $N_2 = 0$). Size quantized band (*1*) would be twice degenerated without the action of a magnetic field or strain. Taking into account the above subbands of the size quantized zone, one can explain peculiarities of magneto-resistance dependence in InSb whiskers on application of the longitudinal magnetic field (Fig. 3).

Let us consider three cases.

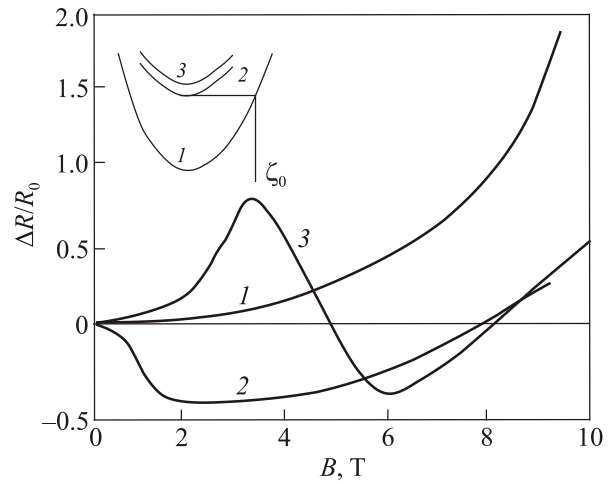(a) A chemical potential level without the action of a magnetic field is greatly lower than the bottom of the

Fig. 3. Theoretical dependence of reduced longitudinal magneto-resistance for InSb whiskers. In the inset: schematic representation of quantum subband and position for a chemical potential.

subband that was twice degenerated in this case. At increase of magnetic field intensity the chemical potential ξ_0 decreases monotonously, which is accompanied with a rise of the whisker magnetoresistance (see Fig. 3, curve *1*).

(b) A chemical potential matches or is slightly below the bottom of the second subband. Then with increasing magnetic field *B*, the chemical potential decreases and the magnetoresistance initially decreases and then increases monotonically (Fig. 3, curve *2*).

(c) A chemical potential is slightly above the bottom of the second subband. Then with increasing magnetic field the magnetoresistance first increases and then, when ξ_0 passes the subband bottom, sharply enough falls. With the further increase in the magnetic field, it grows monotonously (Fig. 3, curve *3*).

The last case (Fig. 3, curve *3*) explains quite well the experimental dependence of the magnetoresistance InSb whiskers (see, for example, Figs. 1(a),(b), curve *1*) in small magnetic fields at low temperatures. So, strained and unstrained longitudinal magnetoresistance changes the sign and crosses from positive to negative at various magnetic fields. Exceptions are only the InSb whiskers with doping concentration corresponding to the metal side of MIT. Their longitudinal magnetoresistance for strained samples is positive in all range of the magnetic field (Fig. 2(c), curve *2*). However, still unclear is the cause of size quantization of electrons in the whiskers rather large diameter (of the order of tens of microns).

The observed phenomenon could be explained in other way. Fundamentally, it should be noted that the prevalence of surface conductance in the specimens as compared with bulk one. Thus, the whisker growth by chemical vapor deposition in halogen closed system leads to the increase of dopant impurity approaching the whisker surface. There are various parameters that influence impurity distribution. For instance, gain in impurity doping near the whisker surface

might be caused by diffusion of impurities to the surface during the sample annealing after growth.

Provided the assumption of the pervasiveness of surface conductance in the whisker is accurate, i.e., the main part of charge carriers transport takes place in the subsurface layers of the whisker, which can be characterized by effective wire radial distance dW, it can be concluded that the magnetoresistance peaks in Fig. 2(b) are present as a consequence of the classical size effect, where the wire boundary scattering is reduced as the cyclotron radius becomes smaller than the effective wire radial distance, resulting in a decrease in the resistivity. The same behavior is typical for the magnetoresistance of bismuth nanowires of the diameter range $d_0 = 45$–200 nm, while the peak position B_m varies linearly with $1/dW$ as the wire diameter increases [27]. The possibility of B_m occurring is determined by $B_m \approx 2ck_F/EdW$, where k_F is the wavevector at the Fermi energy [20]. Effective wire radial distance can be calculated taking into account obtained Fermi energy E that for InSb whiskers ranges within $dW \sim 150$ nm. The magnetoresistnace switching may be connected to the electron conductance in thin subsurface layers with effective wire radial distance, much smaller than the carriers' free path $l_e \sim 250$ nm, calculated from the Shubnikov–de Haas oscillation analysis [20]. Therefore, our above consideration of the existence of electron subbands in subsurface layer in the whiskers is probably right. As is shown in Figs. 2(a),(b), the NMR observed for the InSb whiskers above B_m indicates that wire boundary scattering is a dominant process for the longitudinal magnetoresistance, which confirms that carriers' free path is significantly larger than the effective wire radial distance.

4. Conclusions

Longitudinal magnetoresistance of strained and unstrained InSb whiskers with tin concentration $6 \cdot 10^{16}$–$6 \cdot 10^{17}$ cm^{-3} in the vicinity to MIT from insulator and metal side of the transition was studied in the temperature range 4.2–40 K and magnetic field 0–10 T. The Shubnikov–de Haas oscillations were observed in magnetoresistance dependences of n-type conductivity InSb whiskers in all range of magnetic fields. A larger number of longitudinal magnetoresistance peaks at 4.2 K was visible in strained and unstrained samples doped to concentration corresponding metal side of MIT. However, strained InSb whiskers doped to concentration at insulator side of MIT have larger magnetoresistance oscillations than unstrained one.

Longitudinal magnetoresistance of all studied samples, except heavily doped corresponding to the meal side of MIT, was shown to alter its sign with magnetic field increasing: it is positive in the magnetic fields up to 3–8 T depending on doping concentration and it becomes negative at higher magnetic fields.

There have also been discussed possible mechanisms of the large negative magnetoresistance and above mentioned sign switch occurring in the whisker magnetoresistnce. In the most likelihood, the contribution in the origin of large NMR and change of longitudinal magnetoresistance sign in unstrained and strained InSb whiskers could lay in the existence of classical size effect and boundary scattering during conductance in quantized zone of thin subsurface layer of InSb whiskers, respectively.

_____

1. A.K. Walton and J.C. Dutt, *J. Phys. C: Solid State Physics* **10**, L29 (1977).
2. D.G. Hayes, *Semicond. Sci. Technol.* **32**, 085002 (2017).
3. M. Edirisooriya, T.D. Mishima, C.K. Gaspe, K. Bottoms, R.J. Hauenstein, and M.B. Santos, *J. Crystal Growth* **311**, 1972 (2009).
4. B. Bennett, R. Magno, J. Boos, W. Kruppa, and M. Ancona, *Solid State Electron.* **49**, 1875 (2005).
5. C.K. Gaspe, M. Edirisooriya, T.D. Mishima, P.A. Dilhani Jayathilaka, R.E. Doezema, S.Q. Murphy, and M.B. Santos, *J. Vacuum Sci. Technol. B* **29**, 03C110 (2011).
6. P. Chang, X. Liu, L. Zeng, K. Wei, and G. Du, *IEEE Trans. Electron Devices* **62**, 947 (2015).
7. B.R. Bennett, M.G. Ancona, J.B. Boos, and B.V. Shanabrook, *Appl. Phys. Lett.* **91**, 042104 (2007).
8. J.F. Klem, J.A. Lott, J.E. Schirber, S.R. Kurtz, and S.Y. Lin, *J. Electron. Mater.* **22**, 315 (1993).
9. M. Radosavljevic, T. Ashley, A. Andreev, S. Coomber, G. Dewey, M. Emeny, M. Fearn, D.G. Hayes, K.P. Hilton, M.K. Hudait, R. Jefferies, T. Martin, R. Pillarisetty, W. Rachmady, T. Rakshit, S.J. Smith, M.J. Uren, D.J. Wallis, P.J. Wilding, and R. Chau, *IEEE International Electron Devices Meeting* (2008).
10. Y. Li, Z. Wang, Y. Lu, X. Yang, Z. Shen, F. Sheng, C. Feng, Yi Zheng, and Z.-A. Xu, *Front. Phys.* **12**, 127205 (2017).
11. J.B. Webb, M. Paiment, and T.S. Rao, *Solid State Commun.* **71**, 871 (1989).
12. S. Ishida, K. Takeda, A. Okamoto, and I. Shibasaki, *Phys. Status Solidi (c)* **2**(8), 3067 (2005).
13. K. Imamura, K. Haruna, and I. Ohno, *Jpn. J. Appl. Phys.* **19**(3), 495 (1980).
14. A. Kochura, B. Aronzon, M. Alam, A. Lashkul, S. Marenkin, M. Shakhov, E. Kochura, and E. Lahderanta, *J. Nano- and Electronic Phys.* **5** (4), 04015 (2013).
15. S. Gardelis, J. Androulakis, Z. Viskadourakis, E.L. Papadopoulou, J. Giapintzakis, S. Rai, G. Lodha, and S. Roy, *Phys. Rev. B* **74**, 214427 (2006).
16. J.A. Peters, N.D. Parashar, N. Rangaraju, and B.W. Wessels, *Phys. Rev. B* **82**, 205207 (2010).
17. N. Parashar, N. Rangaraju, V. Lazarov, S. Xie, and B. Wessels, *Phys. Rev. B* **81**, 115321 (2010).
18. L. Lari, S. Lea, C. Feeser, B.W. Wessels, and V.K. Lazarov, *J. Appl. Phys.* **111**, 07C311 (2012).
19. J. Liu, M.P. Hanson, J.A. Peters, and B.W. Wessels, *ACS Appl. Mater. Interfaces* **7**, 24159 (2015).

20. A. Druzhinin, I. Ostrovskii, Yu. Khoverko, N. Liakh-Kaguy, I. Khytruk, and K. Rogacki, *Materials Research Bulletin* **72**, 324 (2015).

21. A. Druzhinin, I. Ostrovskii, Yu. Khoverko, and N. Liakh-Kaguy, *Fiz. Nizk. Temp.* **42**, 581 (2016) [*Low Temp. Phys.* **42**, 453 (2016)].

22. A. Druzhinin, I. Ostrovskii, Yu. Khoverko, N. Liakh-Kaguy, and K. Rogacki, *Fiz. Nizk. Temp.* **44**, 1521 (2018) [*Low Temp. Phys.* **44**, 1189 (2018)].

23. A. Druzhinin, I. Ostrovskii, Yu. Khoverko, N. Liakh-Kaguy, and Iu. Kogut, *Mater. Sci. Semicond. Processing* **14**, 18 (2011).

24. A. Druzhinin, I. Ostrovskii, Yu. Khoverko, N. Liakh-Kaguy, and A. Vuytsyk, *Functional Mater.* **21**(2), 130 (2014).

25. A. Druzhinin, I. Ostrovskii, Y. Khoverko, and R. Koretskii, *Mater. Sci. Semicond. Processing* **40**, 766 (2015).

26. I. Maryamova, A. Druzhinin, E. Lavitska, I. Gortynska, and Y. Yatzuk, *Sensors and Actuators A* **85**, 153 (2000).

27. Z. Zhang, X. Sun, M.S. Dresselhaus, J.Y. Ying, J. Heremans, *Phys. Rev. B* **61**, 4850 (2000).

_____

Квантування у магнітоопорі деформованих ниткоподібних кристалів InSb

А. Дружинін, І. Островський, Ю. Ховерко, Н. Лях-Кагуй

На основі досліджень поздовжнього магнітоопору ниткоподібних кристалів InSb n-типу провідності, легованих Sn до концентрацій $6\cdot10^{16}$–$6\cdot10^{17}$ см$^{-3}$, в інтервалі температур 4,2–40 K і магнітних полів до 10 Тл виявлено осциляції Шубнікова–де Гааза в деформованих і недеформованих зразках. Проведено аналіз поведінки польових залежностей магнітоопору згідно відомих теоретичних уявлень. Встановлено, що з підвищенням індукції магнітного поля магнітоопір ниткоподібних кристалів InSb змінює свій знак від позитивного до від'ємного. Обговорюються механізми, які зумовлюють появу високих значень від'ємного магнітоопору (ВМО) у зразках InSb з концентрацією легуючої домішки, що відповідає близькості до переходу метал–діелектрик. Існування ВМО пов'язане з класичним розмірним ефектом, а також гранічним розсіюванням у провідності приповерхневих шарів мікрокристалів.

Ключові слова: ниткоподібні кристали InSb, від'ємний поздовжній магнітоопір, концентрація домішки, вплив деформації.

Квантование в магнитосопротивлении деформированных нитевидных кристаллов InSb

А. Дружинин, И. Островский, Ю. Ховерко, Н. Лях-Кагуй

На основе исследований продольного магнитосопротивления нитевидных кристаллов InSb n-типа проводимости, легированных Sn до концентраций $6\cdot10^{16}$–$6\cdot10^{17}$ см$^{-3}$, в интервале температур 4,2–40 K и магнитных полей до 10 Тл обнаружены осцилляции Шубникова–де Гааза в деформированных и недеформированных образцах. Проведен анализ поведения полевых зависимостей магнитосопротивления согласно известным теоретическим представлениям. Установлено, что с повышением индукции магнитного поля магнитосопротивление нитевидных кристаллов InSb меняет свой знак от положительного к отрицательному. Обсуждаются механизмы, которые обусловливают появление высоких значений отрицательного магнитосопротивления (ОМС) в образцах InSb с концентрацией легирующей примеси, соответствующей близости к переходу металл–диэлектрик. Существование ОМС обусловлено классическим размерным эффектом, а также граничным рассеиванием в проводимости приповерхностных слоев микрокристаллов.

Ключевые слова: нитевидные кристаллы InSb, отрицательное продольное магнитосопротивление, концентрация примеси, влияние деформации.